Electronic Supplementary Material (ESI) for Materials Advances.

Supplementary Information:

Thermoelectric property enhancement of single-wall carbon nanotube network by ICl intercalation and filling: A first-principles study†

Md. Mafizul Islam[1,2] and Ahmed Zubair[1,*]

[1]Department of Electrical and Electronic Engineering, Bangladesh University of Engineering and Technology, Dhaka 1205, Bangladesh.

[2]Department of Textile Machinery Design and Maintenance, Bangladesh University of Textiles, Dhaka 1208, Bangladesh.

[*]ahmedzubair@eee.buet.ac.bd

S1 Initial and Optimized Structures of ICl-doped SWCNT bundles

We presented the initial and optimized geometry of the ICl-doped SWCNT network in Figure S1. For doping inside the tube, the initial structures were built with three ICl molecules placed vertically in close spacing (C1) and at a distance (C2) between adjacent dopants. The optimized geometry resulted in an I_2Cl and one ICl_2 compound since charge-sharing phenomena took place between them, as depicted in Figures S1(a) and (b). The intercalation of ICl molecules outside the tube horizontally oriented dopants in close spacing (C3) resulted in weak covalent bonds between the dopant atoms due to a small amount of charge sharing, while the bond was strong when the ICl molecules were far from their neighbors (C4), as can be seen in Figures S1(c) and (d). The ICl molecules formed a chain when they were in the vertical orientation (C5 and C6) (see Figures S1(e) and (f)).

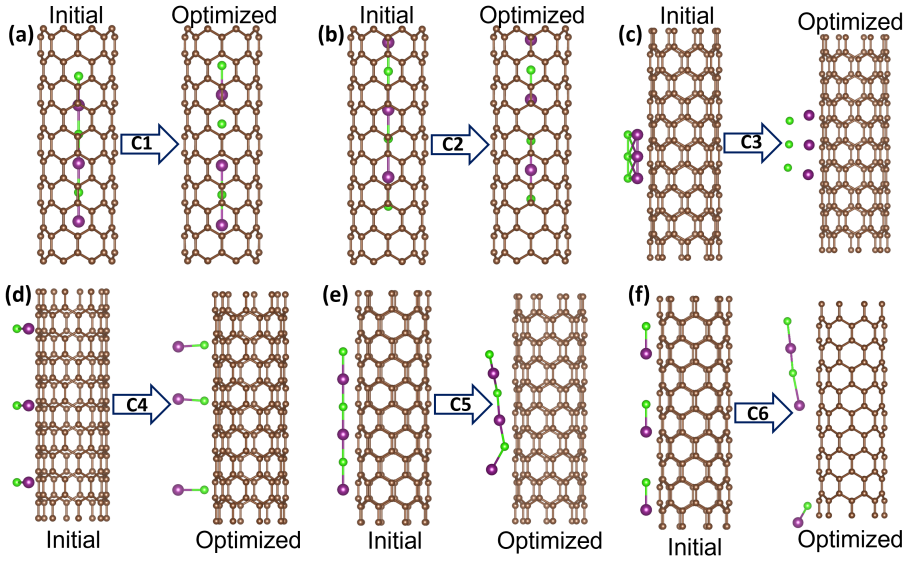

Figure S1: Initial and final structures of ICl doped SWCNT bundles for (a) configuration C1, (b) configuration C2), (c) configuration C3, (d) configuration C4, (e) configuration C5, and (f) configuration C6.

S2 Band structure of pristine (8,0) SWCNT

We calculated the band structure of the pristine (8,0) SWCNT network for the full k-path of the hexagonal Brillouin zone (see Figure S2). Since GGA-PBE functional underestimated the band gap, we calculated and plotted the band structure for hybrid functional in addition to that obtained using GGA-PBE

functional. The hybrid functional-based calculation estimated a 1.1 eV band gap, which is smaller than the reported value for isolated (8,0) SWCNT. Band gap narrowing occurred due to the interaction between neighboring tubes for bundled CNT.

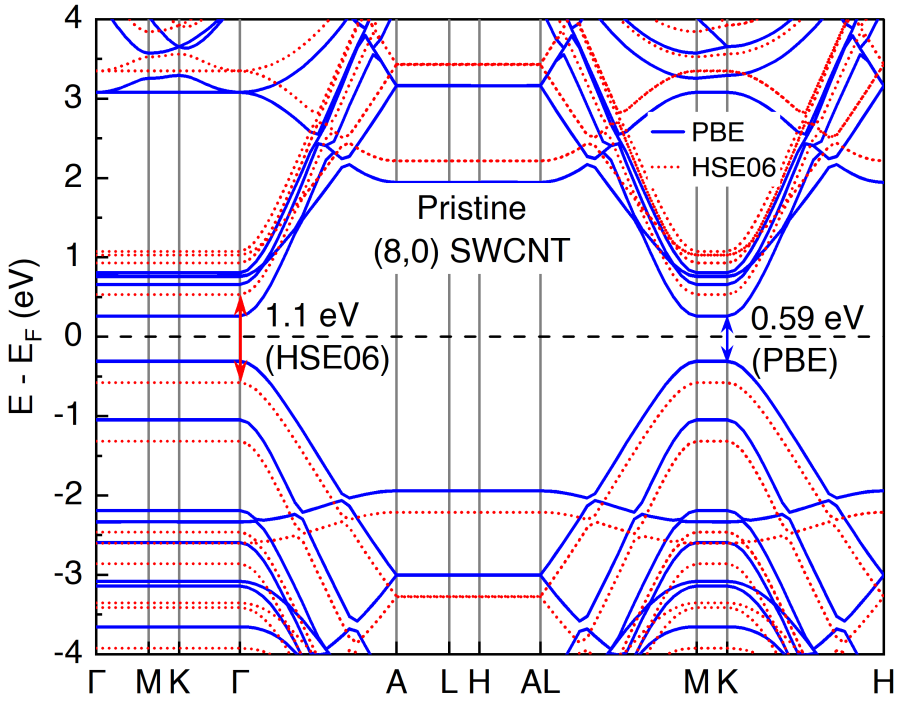

Figure S2: GGA-PBE and hybrid functional (HSE06) band structures of pristine (8,0) SWCNT bundle.

S3 Seebeck coefficient at elevated temperature

We calculated the Seebeck coefficient beyond 1000 K particularly for the C1 doping configuration. The effect of bipolar transport, however, was more noticeable and resulted in a considerable decrease of S with even sign reversal beyond 1650 K, as observed in Figure S3. At lower temperatures, S had a larger value. The S dropped when the temperature rose, primarily because of dominance of bipolar transport. Because thermal stimulation caused minority carrier production, bipolar transport was significantly higher at high temperatures with low carrier concentrations. Additionally, there are relatively fewer unoccupied states above the Fermi level at high temperatures, preventing carriers from jumping to upper energy states. The combined effect of these occurrences resulted in a drop of Seebeck coefficient at high temperatures.

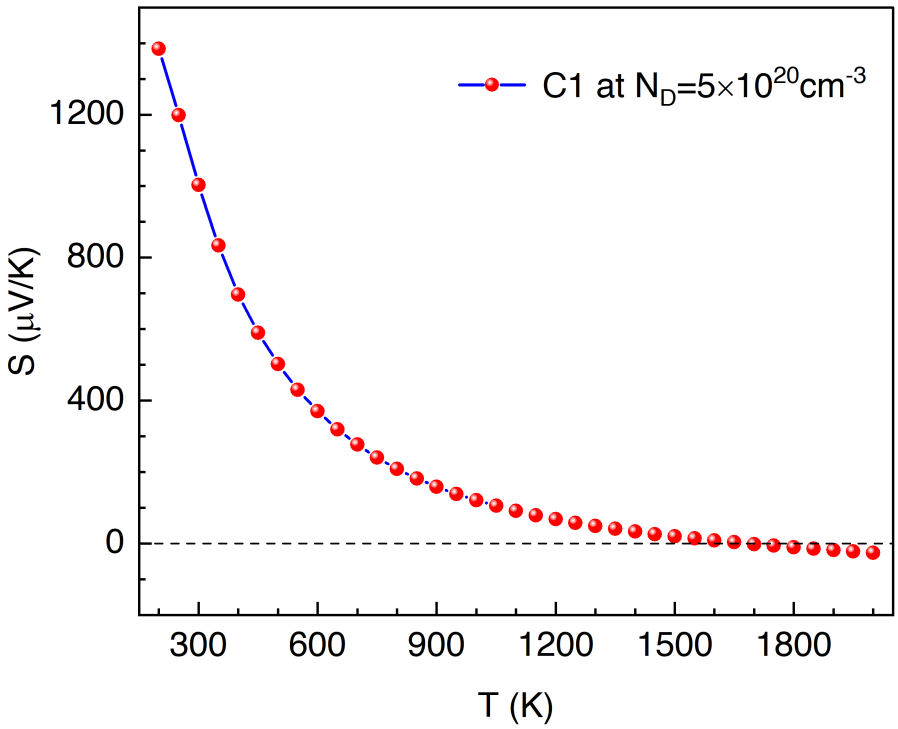

Figure S3: The peak of the Seebeck coefficient variation with temperature for C1 configuration.

S4 Doping concentration-dependent thermoelectric property of ICl-doped SWCNT bundle

We systematically calculated S, σ, and PF at different doping concentrations of ICl onto the SWCNT bundle at room temperature and plotted in Figure S4. Firstly, we intercalated ICl molecules closely spaced in horizontal orientation (C3) between adjacent SWCNTs of 1×1×5 supercell size and varied the number of ICl molecules from one to ten. The pristine SWCNT supercell contained 160 atoms and two additional atoms were added for each ICl molecule. The ICl concentration was calculated as the atomic percentage of dopants (at. %), a percentage of the number of dopant atoms with respect to total number of atoms on the doped system. All the convergence and computational parameters were chosen as adopted in the main manuscript. The increased a bit with increase of ICl concentration till it reached 9.09%, due to origination of impurity bands which increased the number of quantum channel for electronic transport and the increased number of electronic states at the edge and below the valence band, where the E_F was roaming around because of varying ICl concentration. The lifted sharply to14.45 kSm^{-1} when the ICl concentration increased to

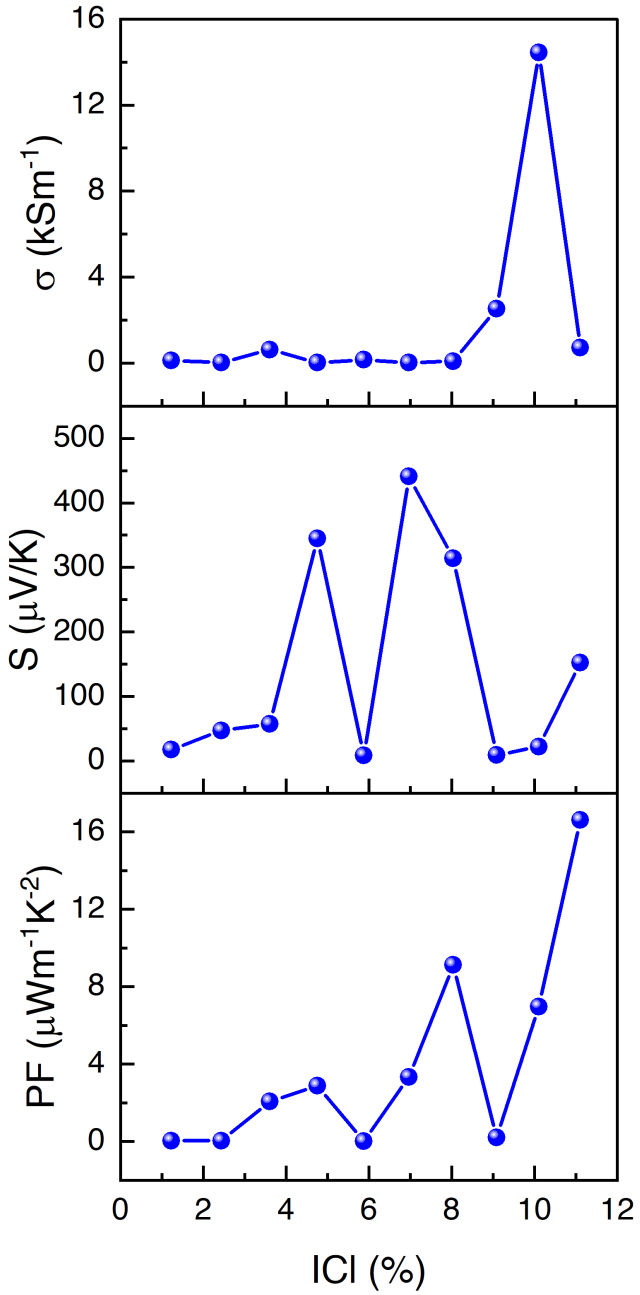

Figure S4: The dopant concentration dependent electrical conductivity σ, Seebeck coefficient S, and thermoelectric power factor at 300 K temperature.

10.11%. Further increase of ICl concentration (11.11%) increased with a little amount. This peak of with ICl concentration was due to the presence of van Hove Singularities (VHS) in the DOS of one-dimensional material, where a sharp peak in DOS was happening intermittently. The Seebeck coefficient increased a little amount ($\sim 57\ \mu V K^{-1}$) till the ICl concentration reached 3.61 %. The collective result of impurity band formation, increase of DOS at the E_F, increase of carrier concentration and E_F shifting due to ICl doping reduced the Seebeck coefficient, since S is inversely proportional to carrier concentration. However, above 3.61% of ICl concentration, the value of S found different at different doping concentration. The S at the Fermi level depends on the slope of DOS and consequently on energy dependent $\sigma(\epsilon)$ as well, according to the Mott's formula[1], S can be expressed as

$$S\left(\epsilon, T\right) = \frac{\pi^2 k_B^2 T}{3e}\left(\frac{\partial \ln\left(\sigma\left(\epsilon\right)\right)}{\partial \epsilon}\right)_{\epsilon=\epsilon_F}$$

Where, $\sigma\left(\epsilon\right)$ is the energy-dependent electrical conductivity. S can further be elaborated in terms of DOS $N\left(\epsilon\right)$ and carrier mobility $\mu\left(\epsilon\right)$.[2]

$$S\left(\epsilon, T\right) = \frac{\pi^2 k_B^2 T}{3e}\left(\frac{1}{N\left(\epsilon\right)}\ \frac{\partial N\left(\epsilon\right)}{\partial \epsilon} + \frac{1}{\mu\left(\epsilon\right)}\ \frac{\partial \mu\left(\epsilon\right)}{\partial \epsilon}\right)_{\epsilon=\epsilon_F}$$

The reason for not having any specific trend of S with varying ICl concentration might be due to the collective impact of both DOS and carrier mobility. The drastic increment of S at some ICl concentration might have occurred, possibly due to shift of E_F at an energy level where the slope of DOS was higher. The overall effect of both S and contributed to the power factor according to $S^2\sigma$. The PF was a bit lower till the ICl concentration of 3.61%. However, the lower value of PF ($2.87\ \mu W m^{-1} K^{-2}$) at 4.76% ICl concentration despite higher value of S ($345\ \mu V K^{-1}$) was due to a very small ($24\ S m^{-1}$). A high PF of $\sim 16.6\ \mu W m^{-1} K^{-2}$ was obtained for 11.11% ICl concentration due to a decent value of both S and at the Fermi level.

References

[1] M. Jonson and G. D. Mahan, *Phys. Rev. B*, 1980, **21**, 4223–4229.

[2] G. Prunet, F. Pawula, G. Fleury, E. Cloutet, A. Robinson, G. Hadziioannou and A. Pakdel, *Materials Today Physics*, 2021, **18**, 100402.